Journal of Nuclear Materials 465 (2015) 793–804

Contents lists available at ScienceDirect

Journal of Nuclear Materials

journal homepage: www.elsevier.com/locate/jnucmat

Spatial variability in the coefficient of thermal expansion induces pre-service stresses in computer models of virgin Gilsocarbon bricks

José David Arregui-Mena [a], Lee Margetts [a,*], D.V. Griffiths [b], Louise Lever [c], Graham Hall [a], Paul M. Mummery [a]

[a] School of Mechanical, Aerospace, and Civil Engineering, University of Manchester, Oxford Road, Manchester, M13 9PL, UK
[b] Colorado School of Mines, 1500 Illinois St, Golden, CO 80401, USA
[c] Research Computing, University of Manchester, Oxford Road, Manchester, M13 9PL, UK

ARTICLE INFO

Article history:
Received 1 October 2014
Received in revised form
12 May 2015
Accepted 16 May 2015
Available online 9 June 2015

Keywords:
Gilsocarbon
Nuclear graphite
Finite element method
Monte Carlo Simulation
Modelling

ABSTRACT

In this paper, the authors test the hypothesis that tiny spatial variations in material properties may lead to significant pre-service stresses in virgin graphite bricks. To do this, they have customised ParaFEM, an open source parallel finite element package, adding support for stochastic thermo-mechanical analysis using the Monte Carlo Simulation method. For an Advanced Gas-cooled Reactor brick, three heating cases have been examined: a uniform temperature change; a uniform temperature gradient applied through the thickness of the brick and a simulated temperature profile from an operating reactor. Results are compared for mean and stochastic properties. These show that, for the proof-of-concept analyses carried out, the pre-service von Mises stress is around twenty times higher when spatial variability of material properties is introduced. The paper demonstrates that thermal gradients coupled with material incompatibilities may be important in the generation of stress in nuclear graphite reactor bricks. Tiny spatial variations in coefficient of thermal expansion (CTE) and Young's modulus can lead to the presence of thermal stresses in bricks that are free to expand.

1. Introduction

1.1. Objectives

The principal objective of this paper is to report on work carried out to test the hypothesis that tiny spatial variations in material properties may lead to significant pre-service stresses in virgin graphite bricks. Unrestrained temperature expansion with uniform mean material properties will not produce substantial stresses. However, unrestrained temperature expansion with more realistic random material properties could produce stresses that are currently ignored in thermo-mechanical engineering simulations. The authors also report on modifications made to open source parallel finite element software, adding functionality to generate spatially random fields for coefficient of thermal expansion (CTE) and Young's modulus. As the use of open source software is not common in nuclear engineering, we also describe in detail how the software was tested.

1.2. Background

Most of the UK nuclear reactors use graphite as a moderator. The main function of the graphite components is to moderate the nuclear reactions and to provide channels for fuel cooling and control rods entry [1]. The UK currently deploys three types of reactor: Advanced Gas-cooled Reactors (AGRs), Magnox Reactors and Pressurised Water Reactors (PWR). The fleet of 14 AGRs and the remaining Magnox reactor still in operation are graphite moderated.

During the lifetime of a graphite moderated reactor it is essential to ensure the integrity of the graphite core. Distortions, cracking and weight loss in the graphite components can potentially prevent normal reactor operations such as the loading and unloading of fuel or control rods. Dimensional changes and cracking may also impede the correct circulation of coolant. Damage to the graphite core could reduce the lifetime of a nuclear reactor. The graphite moderator bricks cannot be replaced [2], making the graphite core

* Corresponding author.
E-mail addresses: jose.arreguimena@postgrad.manchester.ac.uk (J.D. Arregui-Mena), lee.margetts@manchester.ac.uk (L. Margetts), d.v.griffiths@mines.edu (D.V. Griffiths), louise.lever@manchester.ac.uk (L. Lever), graham.n.hall@manchester.ac.uk (G. Hall), paul.m.mummery@manchester.ac.uk (P.M. Mummery).

http://dx.doi.org/10.1016/j.jnucmat.2015.05.058
0022-3115/

a critical component of a nuclear power station [3]. It is important to note that graphite component cracking is not a safety issue in itself as long as the core can still perform its function under all operating conditions. That is, the fuel can be adequately cooled, the reactor safely shut down, and the fuel safely removed.

When in-service, graphite is subjected to fast neutron irradiation and oxidation. These phenomena cause a progressive degeneration of the graphite material. Neutron irradiation affects graphite in several ways; it changes the material properties of graphite and causes change in dimensions. In addition to this, neutron irradiation promotes 'irradiation creep' that relieves internal stresses. Graphite used in nuclear reactors can experience two oxidation mechanisms: thermal oxidation and radiolytic oxidation. Thermal oxidation is negligible at normal AGR and Magnox operating temperatures. Radiolytic oxidation is present during the normal operation of an AGR and Magnox reactor and causes considerable weight loss if it is not controlled properly.

Several techniques are used to predict the health of a reactor including direct inspections, measurements taken during the operation of a reactor and computational modelling. Periodic inspections track the ageing effects on graphite caused by nuclear irradiation. A device explores the surface of the graphite core to measure the dimensions and ovality of the channels formed by the graphite bricks and a camera records the condition at the bore. Graphite samples are extracted from the graphite components during fuelling operations and ageing is quantified experimentally, providing insight about the condition of the reactor [2]. Computer modelling is used to predict the structural integrity of the graphite bricks by estimating stresses generated by elastic, thermal, creep and irradiation strains. Modelling is verified by comparing predictions with data from inspections.

1.3. Computer modelling

In the literature, computer modelling focuses on the development and implementation of constitutive equations that capture the full complexity of the physical processes acting on the graphite. For example, Tsang and Marsden [4] [5] have developed Abaqus material user subroutines for Magnox and AGR. In the case of High Temperature Gas-cooled Reactors (HTGR) Mohanty et al. [6] have developed a constitutive model for stress analysis of prismatic graphite bricks. Yu et al. present a microstructure-based model that predicts the lifetime of an HTGR [7].

To date, computer modelling has given important insights into the behaviour of nuclear graphite. However, as is typical in engineering simulation, the output of the models does not match well enough with observations to allow accurate predictions. Operators and regulators cannot yet use simulation alone to assess the maximum period of time a particular reactor can remain in service under safe operating conditions.

One route to improved simulation is to increase the complexity of the constitutive models and increase the temporal and spatial resolution of the finite element meshes. In this paper, the authors instead focus on potential improvements from a different perspective: introducing realism into the definition of material properties in the finite element model.

It is common practice to use a mean value of a material property in an engineering simulation. For example, in a mesh of a graphite brick, all the elements that represent graphite are often given the mean Young's modulus, the mean Poisson's ratio and the mean CTE. These values change as the analysis proceeds when the effects of temperature, irradiation and oxidation are taken into account. The starting point for the analysis is perfect uniformity in the material and any temperature change will lead to expansion without the generation of significant stresses. In contrast, tiny spatial variations in material properties (that exist in graphite bricks before they are brought into service) can induce thermo-elastic strains during a simple temperature change. These pre-service stresses may be an important, but overlooked starting point for simulations that seek to predict how the brick will respond to in-service conditions during the lifetime of the reactor. The most appropriate initial conditions for a simulation may not be uniform material and zero stress during a temperature change.

1.4. Spatial variation in material properties

Spatial variations in material properties, documented in pre-service virgin nuclear graphite [8–14], are related to the properties of the main components used (filler, binder and flour), their arrangement and the method of manufacture. Several types of nuclear graphite have been created for the different needs, stages and generations of nuclear reactor. Pile Grade A (PGA), an anisotropic graphite, was manufactured for the first generation of British reactors, the Magnox reactors. PGA filler particles were obtained from the cracking process in the petroleum industry. The filler particles in PGA have needle shape forms that become preferentially aligned during the extrusion stage of the manufacturing process. This gives the material a direction dependent microstructure and consequentially direction dependent properties. Gilsocarbon, a type of graphite that is quasi-isotropic, is used in AGRs. PGA and Gilsocarbon binders are randomly orientated and thus do not have any preferential alignment [9].

The material properties of the graphite components of AGRs are recorded in heat certificates. A heat certificate is an official document issued by the manufacturer which is linked to a particular batch of components. These records are one of the most important sources of information for the unirradiated material properties of the Gilsocarbon actually used in the construction of the AGRs. A statistical analysis that compared the variation of material properties with the information present in the heat certificates was reported by Preston [13]. This report compares the available material property data for different types of graphite used in nuclear power stations. The statistical analysis shows that there is a significant variation in properties between the graphite bricks used at the various AGRs.

A study of the variability of material properties within a single billet used in the Heysham 2 and Torness reactors was also reported by Preston [14]. A block of Gilsocarbon was divided into three different sections from which 343 specimens were cut and subjected to 12 types of measurement. This report shows that the values of some material properties, such as strength and Young's modulus, vary according to where the samples were taken. Similarly a study of PPA graphite [15], a semi-isotropic extruded graphite similar to Gilsocarbon, also looked at the spatial variability of two billets. The results of a series of four point bend tests indicate a difference of strength of the billet through its length, especially at the ends of the billets. Samples taken from a top section of a billet were on average 11.9% stronger than those from the bottom.

Spatial variation of material properties has also been studied for the next generation of graphite moderator reactors. Variability in strength within a billet has been reported for grade H-451 nuclear graphite [16]. In this study, it was found that the strength of the billets was higher at the edges than in the central core. Kennedy [11] used non-destructive techniques to investigate variations in the Young's modulus, shear modulus and strength in billets of 3 different grades of graphite, namely Stackpole 2020, Union Carbide TS1792 and Toyo Tanso IG11. This study concluded that the mean values were different between billets of the same grade. Carroll, Lord et al. [10] also characterise variability in properties for the NBG-18 graphite grade.

1.5. Stochastic Monte Carlo Simulation

To test the proposed hypothesis (see sub-section 1.1), it is necessary to compare the results of simulations which use mean values with those where there are tiny spatial fluctuations in the properties. Although the latter requires the use of a random field generator, this does not mean that the fluctuations are random; the spatial variation is generated using statistical parameters that are derived experimentally. Solutions to finite element analyses where variability is introduced using random fields are instances of possible outcomes rather than a fixed output, which matches quite well with reality as a hundred graphite bricks submitted to the same experimental test would not respond in exactly the same way. Experimentally, statistics are used to interpret the results, and so with stochastic simulations it is natural that interpretation is not "deterministic".

There are many different variants of stochastic finite element analysis. These are reviewed elsewhere [17]. In this work, the Monte Carlo Simulation (MCS) approach has been used. This allows the engineer to run "deterministic" analyses for many randomly configured models without needing to make any modifications to existing finite element programs. MCS is not currently well supported in commercial software. There are various practical difficulties to overcome such as assigning individual material property values to individual finite elements in a mesh. Typically commercial software expects the creation of a new part for each new material. User interfaces are not set up to handle as many parts as there are elements. Another issue is that randomly generated fields of properties destroy symmetry. Whilst the geometry of a model might be symmetrical, the distribution of properties is not. This means that full three-dimensional models need to be employed substantially increasing the number of degrees of freedom that need to be used. Finally, MCS requires repeating essentially the same analysis many times, each slightly different from the other. For this reason, the authors have adopted two open source software platforms, ParaFEM (http://parafem.org.uk) [18] and RFEM (www.engmath.dal.ca/rfem/) [19,20] to carry out this work. ParaFEM is a parallel finite element solver and RFEM is a package for generating random fields of properties for stochastic MCS.

2. Methods

This section outlines how the Stochastic Monte Carlo Simulations were performed and the method used to generate the random fields. It also describes the customisations that were carried out to add random field generation and thermo-mechanical stress analysis to ParaFEM. Finally, details are given regarding the "proof of concept" virtual experiments that were carried out to test the hypothesis that material variability may lead to pre-service stresses in a virgin Gilsocarbon graphite brick.

2.1. Stochastic Monte Carlo Simulation methodology

A typical stochastic MCS procedure, which is concerned with spatial variability of material properties only, is described in the five steps below. The procedure is also illustrated in Fig. 1.

1. **Characterise the material.** The first step is to carry out the necessary experiments to characterise the stochastic nature of the variable of interest.
2. **Determine values for the statistical parameters.** The data gathered are used to calculate the required statistical parameters to describe the nature of the system. The statistical parameters used here are the mean, variance and spatial correlation length of the CTE. The spatial correlation length describes the distance over which the spatially random values would tend to be significantly correlated in the underlying Gaussian field, i.e. reproduce a similar Gauss curve to the one defined by the input mean and variance of the CTE.
3. **Create realisations of the random fields.** The statistical variables are used as input to a random field generator which assigns each finite element in the mesh with a statistically determined valued for CTE. For the results shown in this paper, 100 realisations (Monte Carlo trials using different random fields) were used.
4. **Solve the finite element problem.** The finite element problem is solved using a standard deterministic solver and the response variables (here displacement and stress) are recovered.
5. **Process the results.** The previous two steps are repeated until a convergence criterion is achieved. In order to check the convergence of the analysis the displacements of all the realisations carried out so far are averaged and compared against the deterministic solution. When the averaged values of the displacements return the deterministic output of the deterministic analysis, the algorithm is stopped. When the MCS has been completed, the statistical information is analysed.

2.2. Local Average Subdivision method

The Local Average Subdivision (LAS) method [21] was chosen to generate the random fields for the CTE. The LAS method is based on the idea that most of the engineering measurements are local averages of the measurements of a mechanical material property. It takes into account the "scale effect" and the influence of the size of the samples taken to determine the mechanical material properties of a material. Furthermore, the size of the elements and mesh do not affect the local averaging process of the random field. When the element size of the mesh is changed the statistics related to the averaging process will change in the same fashion. Therefore, the finite element analyst is allowed to choose an appropriate resolution of mesh.

A description of how the algorithm works is given next. Although the authors use a three-dimensional field, it is easier to explain how the LAS method works by considering the two-dimensional case. An initial value of the selected random variable is calculated from the statistics that represent the random process (mean, variance and correlation length) and is assigned to a parental cell with the value Z_1^i, being $I = 1, 2, \ldots$, the number of parental cells. The parental cell is subdivided into four child cells being locally described at each parental cell by the symbol Z_j^{i+1}, where $j = 1, 2, 3, 4$. Fig. 2 illustrates part of the process of the LAS method. The process of subdivision is only presented for cell Z_5^i (although all the cells are eventually subdivided by the LAS method).

The values for each step $\mathbf{Z}^{i+1}$ are distributed as a vector that may be represented in a column vector notation as $Z^i + 1 = \{Z_1^{i+1} + Z_2^{i+1} \cdot Z_3^{i+1} + Z_4^{i+1}\}$. These values are calculated by adding the mean value of the variable of interest to a random value. Each value of a child cell maintains a relationship with the surrounding parent values through a set of covariance matrices. For a more detailed description of the LAS method, see e.g. Griffiths and Fenton [20].

In three dimensions, the process is essentially the same and typical random fields are shown in Fig. 3, highlighting the effect of correlation length on the distribution of CTE values for a cube with side lengths of 48 mm and uniform hexahedral elements of side 1 mm. The correlation length can be obtained experimentally by measuring the physical property of interest at equally spaced locations in the domain and processing that data using statistics

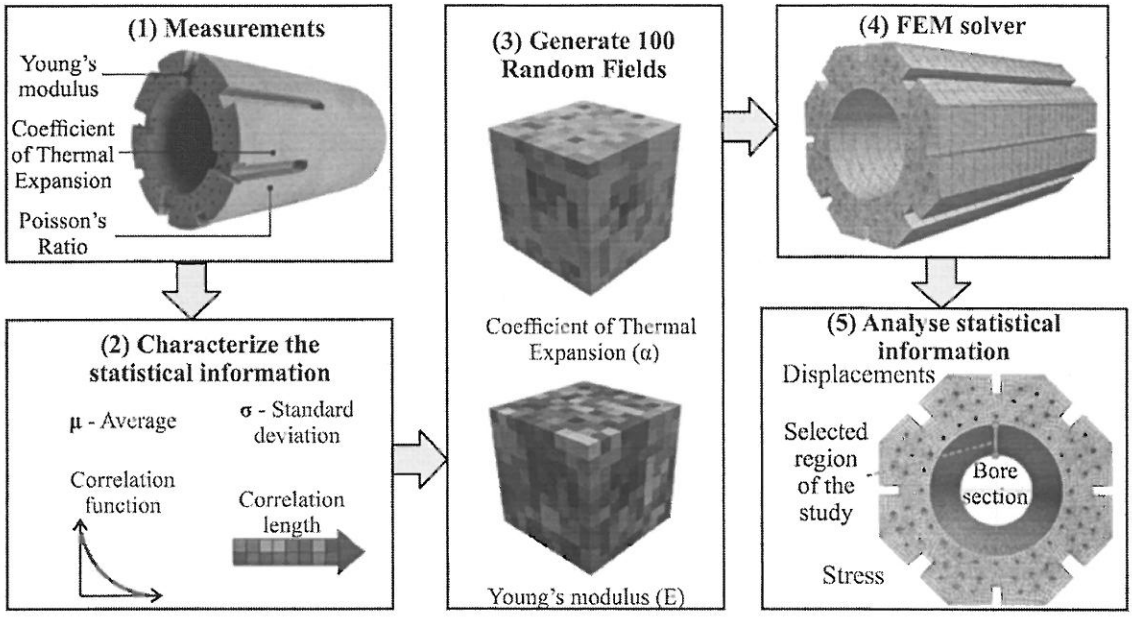

Fig. 1. RFEM steps for the calculation of the circumferential strain and stress in an AGR graphite brick.

[22,23].

The FORTRAN77 subprograms for the LAS method provided with the Fenton and Griffiths textbook [19], namely SIM3D.f and its dependencies, were integrated into the ParaFEM distribution. SIM3D.f creates random fields for cubic domains on a regular grid using input values for mean, variance and correlation length (see Section 2.1 for definitions). A new ParaFEM driver program called RFEMFIELD maps these random fields onto arbitrary meshes such as the nuclear graphite brick. The mapping process works as follows. First, a random field is created for the smallest cube that can envelope the mesh. Boolean operations are then used to identify where the field and the mesh overlap and the field outside the brick is discarded. The random field values are then mapped onto the elements of the mesh. Where more than one field element maps to one mesh element, the field values are averaged. If a field element maps onto more than one mesh element, the same field value is given to those elements. This strategy is heuristic and the best results are obtained when the elements in the mesh are of a similar size and in a similar spatial location to the elements in the random field mesh.

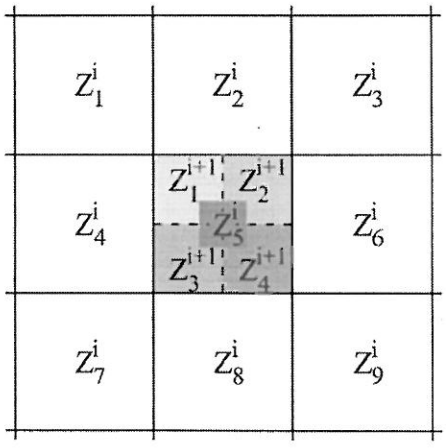

Fig. 2. Two-dimensional case of the Local Average Subdivision (LAS) method.

2.3. Implementation of thermo-elasticity in ParaFEM

Once the random field has been applied to the model, the resulting finite element problem needs to be solved. Here we use ParaFEM. ParaFEM is an open source package for general purpose parallel finite element analysis. It comprises a core library that is used by around 70 driver programs. These cover a broad range of engineering analyses. Implicit problems with a billion unknowns have been solved using up to 32,000 cores on modern supercomputers.

Support for three-dimensional thermo-elasticity was added by the authors by modifying the base program 5.5 from Smith, Griffiths and Margetts [18]. Program 5.5 solves problems in 2D thermo-elasticity. The new driver program was named RFEMSOLVE to be consistent with the RFEMFIELD program described in the previous section. The constitutive equations implemented are described in this section.

The basic equation for static equilibrium problems in the finite element method has the form:

$$\{F\} = [k]\{u\} \tag{1}$$

where {F} is a force vector, [k] is the stiffness matrix and {u} is a vector that contains the displacement components. Let x, y, z be the variables that represent the three spatial dimensions of a Cartesian coordinate system. The relationships between strains and displacements are given by:

$$\varepsilon_x = \frac{\delta u}{\delta x} \quad \varepsilon_y = \frac{\delta v}{\delta y} \quad \varepsilon_z = \frac{\delta w}{\delta z} \quad \gamma_{xy} = \frac{\partial \mu}{\partial y} + \frac{\partial v}{\partial x} \quad \gamma_{yz} = \frac{\partial v}{\partial z} + \frac{\partial w}{\partial y} \quad \gamma_{zx} = \frac{\partial w}{\partial x} + \frac{\partial u}{\partial z} \tag{2}$$

In this case the total strains only involve the thermal strains $\{\varepsilon_{th}\}$.

The stiffness matrix [k] for a single element is formed by:

$$[k] = \int_V [B]^T [D][B] dV \tag{3}$$

The [B] matrix is calculated by differentiating the shape functions according to the elastic theory for the three-dimensional strain field previously shown in the set of Equation (2). [D] is the property matrix calculated from the material properties of the material.

$$[D] = \frac{E}{(1+\nu)(1-2\nu)} \begin{bmatrix} 1-\nu & \nu & \nu & 0 & 0 & 0 \\ \nu & 1-\nu & \nu & 0 & 0 & 0 \\ \nu & \nu & 1-\nu & 0 & 0 & 0 \\ 0 & 0 & 0 & \frac{1-2\nu}{2} & 0 & 0 \\ 0 & 0 & 0 & 0 & \frac{1-2\nu}{2} & 0 \\ 0 & 0 & 0 & 0 & 0 & \frac{1-2\nu}{2} \end{bmatrix} \tag{4}$$

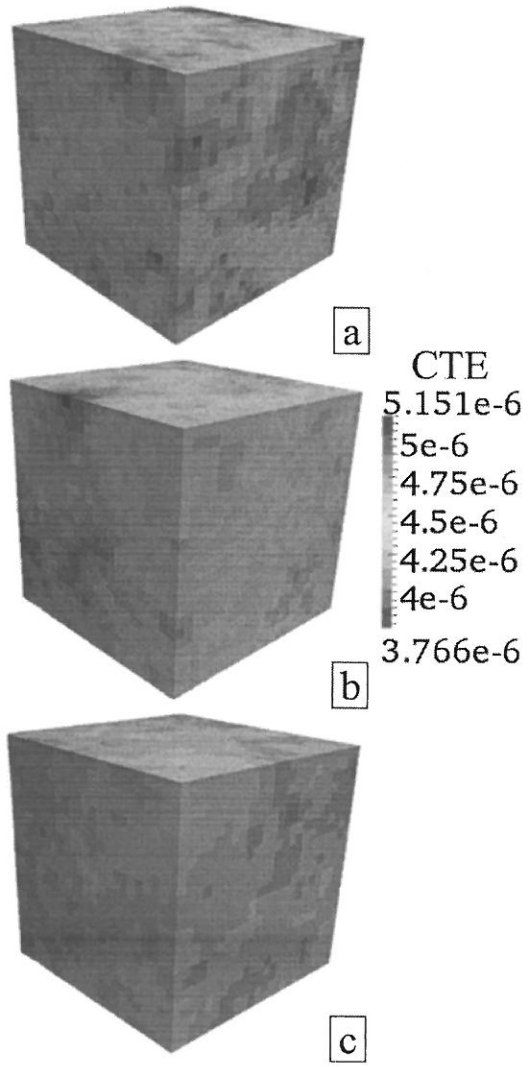

Fig. 3. The correlation length statistically correlates the values of a random variable across a certain distance. In these cases cubes with sides of 24 mm shows the effect of different correlation lengths on CTE values. (a) Correlation length of 12 mm, (b) Correlation length of 24 mm and (c) Correlation length of 48 mm.

The [D] matrix for isotropic materials is determined by the Young's modulus E and the Poisson's ratio ν. The [D] matrix is obtained by different means for the deterministic and stochastic cases. In the deterministic case, a single value for each material property is assigned to all the elements. In the stochastic case, different values are assigned according to a random field.

The force vector {F} for the thermo-elasticity is given by Equation (5):

$$\{F\} = [B]^T [D]\{\varepsilon_0\} dV \tag{5}$$

The vector $\{\varepsilon_0\}$ in Equation (5) represents the thermal strains and is expanded as (6):

$$\{\varepsilon_0\} = \Delta T \begin{Bmatrix} \alpha_x \varepsilon_x \\ \alpha_y \varepsilon_y \\ \alpha_z \varepsilon_z \\ \gamma_{xy} \\ \gamma_{yz} \\ \gamma_{zx} \end{Bmatrix} \tag{6}$$

Terms ε_x, ε_y, ε_z, are the normal strains and γ_{xy}, γ_{yz}, γ_{zx} are the shear strains [24]. In this case, the values of the shear strains (γ_{xy}, γ_{yz}, γ_{zx}) are zero because the thermal expansion only produces a change in volume and not in shape [25]. The scalar values α_x, α_y, and α_z are the coefficients of thermal expansion in the x, y and z directions respectively. As with the values of Young's modulus or Poisson's ratio, the CTE components can be given mean or stochastic values. The temperature change is represented with the symbol ΔT. Program RFEMSOLVE assumes that the temperature change at each nodal point is known.

The source code for the program, documentation and example input data are available from the ParaFEM website (http://parafem.org.uk). The software is available under an open source Berkeley Software Distribution (BSD) license. This is the most permissive type of open source license and allows unrestricted reuse, modification and exploitation of the software.

2.4. Software verification

The correct functioning of the ParaFEM driver program RFEMSOLVE was verified both by comparison with a test problem with a known solution and with the commercial finite element package Abaqus version 6.13-3 [26]. There is no scientific value in

comparing the results of open source software with commercial packages. However, the nuclear industry is known to be very cautious in the adoption of new software and the use of results obtained. It is therefore important to demonstrate that ParaFEM gives comparable results with a software package that is certified for use in the nuclear industry. ParaFEM uses modern software engineering best practice such as a coding standard, a version control system and automated testing. Once initial verification has been carried out and automated tests added, the software can be reliably maintained in the same way as a commercial application.

The analytical problem used for verification concerns the thermal expansion of a brass cube subjected to a homogeneous temperature change. The solution is documented by Davies [27]. The model set up is described in Fig. 4. The cube was discretised into a uniform mesh with 64 quadratic hexahedral elements. The base and two sides were restrained in such a way as to allow the cube to expand uniformly under a homogeneous temperature change. The required material properties were set as follows: CTE = 2.0 E^{-05} mm/mm°C; Young's modulus = 101 GPa and Poisson's Ratio = 0.35 [28]. A uniform temperature rise of 60 °C degrees was applied. The effect of the thermal expansion of the cube is illustrated in Fig. 4.

The displacements calculated at the nodes located at the corners of the cube are given in Table 1 for ParaFEM, Abaqus and the analytical solution. The labels A to H correspond to the location of the nodes as given in Fig. 4. The analytical solution is given by Equation (7) below, where l = length of the side of the cube, α is the CTE and ΔT is the temperature change.

$$u_{th} = l \times \alpha \times \Delta T \tag{7}$$

The solution to the test problem obtained using ParaFEM is in close agreement with both the analytical solution and the Abaqus results (Table 1). The maximum percentage difference between values at the nodes is 0.0016%. This tiny difference can be accounted for by the fact that ParaFEM and Abaqus use two different solvers. ParaFEM uses a parallelised iterative preconditioned conjugate gradient solver [29]. Abaqus uses a direct solver. The 0.0016% difference is less than the stopping criterion set in the iterative solver. Up to the stopping criterion, the results are identical.

More extensive comparisons between Abaqus and ParaFEM were also made for other models with different arbitrary geometries and boundary conditions. Results are not presented here. The effort led to the authors being confident that the software implementation had been carried out correctly.

2.5. Brick geometry, mesh and boundary conditions

Nuclear graphite brick geometry varies between different power stations. In this paper, a brick similar to those in service at the Hinkley Point B AGR was used to perform the analysis. The geometry of the brick was discretised using 91,938 quadratic hexahedral elements, leading to a mesh with 421, 405 nodes. The analysis was carried out using full integration. Mesh sensitivity has not been explored as the purpose of the work is to prove the principle that tiny variations in material properties can generate pre-service stresses.

The boundary conditions applied to the brick were based on the "3-2-1 rule". This set of boundary conditions requires the selection of 3 points that form a plane in space. The first point is constrained in all directions, the second in 2 directions and the third in one direction (Fig. 5). The aim is to eliminate rotations and rigid body motions from the solution space.

In a deterministic analysis (where the same mean CTE is used for all elements), the brick could be restrained using similar boundary conditions to the brass cube discussed earlier. For example, all nodes on the base could be fixed in the Z-direction to set the base as a zero reference point for free deformation in the rest of the model. In a stochastic analysis, where the properties are randomised, restraining all the nodes from moving in a particular direction along a plane would be problematic. The base of the brick, for example, contains adjacent elements with different randomised properties. Unconstrained, each would deform to a different degree and the initial smooth plane would become a surface with tiny, irregular distortions. Constraining all elements on such a plane would lead to stresses arising from the boundary conditions rather than the free thermal expansion of the brick. The minimalistic "3-2-1" rule overcomes these issues.

2.6. Material properties

The values for the material properties selected for the finite element analyses are listed in Table 2. The material is assumed to be virgin isotropic Gilsocarbon graphite. The mean values are used for the deterministic analyses where each finite element in the brick has the same property. Where indicated, the values were obtained from Tsang and Marsden [4]. The values used for standard deviation and correlation length were estimated by the authors for the purpose of testing the hypothesis (sub-section 1.1). Experimental work is needed to define these values.

The material properties for the stochastic MCS analyses were generated using the LAS random field generator described earlier. A unique set of properties is required for each "realisation" of the stochastic MCS simulation. One hundred realisations were carried out, requiring one hundred unique input decks. The number of realisations required is problem dependent. One hundred is the number of realisations whereby the mean of the stochastic MCS

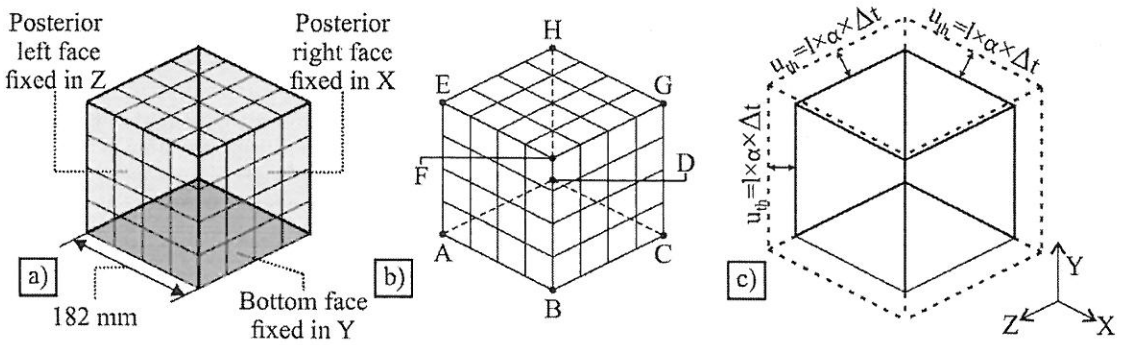

Fig. 4. From left to right: (a) Boundary conditions and dimensions; (b) Location of the nodes where values are compared between the analytical solution, ParaFEM and Abaqus and (c) Original (solid line) and deformed (dashed line) geometry.

Table 1
Displacements calculated using ParaFEM, Abaqus and the analytical solution.

Node	Displacements ParaFEM (mm)			Node	Displacements ParaFEM (mm)		
Label	X	Y	Z	Label	X	Y	Z
A	0	0	2.36E-01	E	0	2.36E-01	2.36E-01
B	2.36E-01	0	2.36E-01	F	2.36E-01	2.36E-01	2.36E-01
C	2.36E-01	0	0	G	2.36E-01	2.36E-01	0
D	0	0	0	H	0	2.36E-01	0
Node	Displacements Abaqus (mm)			Node	Displacements Abaqus (mm)		
Label	X	Y	Z	Label	X	Y	Z
A	−7.53E-32	−7.53E-32	2.36E-01	E	−7.53E-32	2.36E-01	2.36E-01
B	2.36E-01	−7.53E-32	2.36E-01	F	2.36E-01	2.36E-01	2.36E-01
C	2.36E-01	−7.53E-32	−7.53E-32	G	2.36E-01	2.36E-01	−7.53E-32
D	−7.53E-32	−7.53E-32	−7.53E-32	H	−7.53E-32	2.36E-01	−7.53E-32
Node	Displacements analytical solution (mm)			Node	Displacements analytical solution (mm)		
Label	X	Y	Z	Label	X	Y	Z
A	0	0	2.36E-01	E	0	2.36E-01	2.36E-01
B	2.36E-01	0	2.36E-01	F	2.36E-01	2.36E-01	2.36E-01
C	2.36E-01	0	0	G	2.36E-01	2.36E-01	0
D	0	0	0	H	0	2.36E-01	0

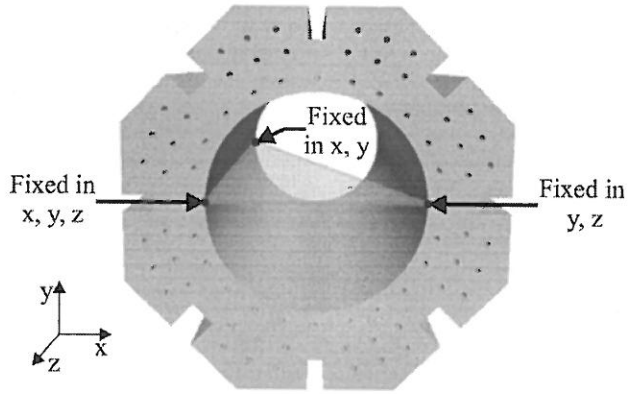

Fig. 5. 3-2-1 Rule boundary conditions.

results is close to the deterministic answer.

The input values used to calibrate the LAS random field generator are the mean, standard deviation and correlation length. The mean values are the same as those used in the deterministic analysis. The standard deviation for the CTE was set to 10% to simulate an extreme case of material variation in Gilsocarbon. The input values used for the Young's modulus (E) were determined using an empirical relationship for virgin graphite between CTE (α) and Young's modulus proposed by Yoda and Fujisaki [30]. Each value of CTE assigned to an element generated by the LAS random field is related to the value of the Young's modulus by Equation (8). Each element therefore has a unique CTE value and unique Young's modulus, E(random).

$$\text{Constant} = \alpha(deterministic) \times \text{E}(deterministic) \tag{8}$$

The values of CTE are then assigned to each element generated by the LAS random field, which are related to the value of the Young's modulus by Equation (9). Each element therefore has a unique CTE (α(random)) value and unique Young's modulus, E(random).

$$\text{E}(random) = \alpha(random)/\text{constant} \tag{9}$$

The spatial variability of the material is represented by the correlation length. The value chosen was governed by the size of the elements in the mesh rather than known values. There is no experimental data available for nuclear graphite and a value of 100 mm has been chosen arbitrarily. The authors emphasise the purpose of this work is to demonstrate the effect of variability in properties rather than make accurate predictions. In a true engineering study, experimental data would be used to determine the typical element size required in the mesh.

2.7. Temperature profiles

Temperature change in graphite components is mainly dependent upon two processes of heat transfer: radiation and convection. The sources of heat that interact with the graphite bricks are the heat generated by the fuel and the heat generated in the graphite components by neutron irradiation. Computer programs are often used to determine the heat generated at the core of a reactor [31]. The estimated temperatures are compared to real reactor data obtained from a few locations measured by thermocouples placed on the graphite bricks. In the case of an AGR the temperature inside the brick is higher than the exterior. The temperature profiles of the bricks also depend upon the position the graphite component occupies in the core [1].

Analyses were carried out for three different temperature profiles. The selected temperature profiles for this study are: a uniform

Table 2
Common values for virgin isotropic graphite.

Material properties of isotropic graphite	Mean values	Standard deviation
Mean coefficient of thermal expansion	4.35×10^{-6} (mm/mm °C) [4]	4.35×10^{-7} (mm/mm °C)
Poisson's ratio	0.2 [4]	
Dynamic Young's modulus	10 GPa [4]	
Correlation length in all directions	100 mm	

temperature change; a temperature change with a linear gradient between the inside and outside surfaces of the brick; and a temperature profile similar to that expected inside a reactor. The uniform temperature change assumes a rise in temperature to 370 °C in all elements of the brick, from a reference temperature of 20 °C. The 350 °C temperature rise produces the thermal strains. For the linear gradient, the brick is heated from a uniform 20 °C to a temperature of 400 °C in the bore of the brick and 300 °C on the exterior surfaces. The "real" profile was estimated from data obtained during routine temperature measurements of the reactor. The reference temperature was again a uniform 20 °C. The 3 temperature profiles are shown in Fig. 6.

2.8. Running the Monte Carlo Simulation

The MCS was run on the UK regional supercomputing facility N8 HPC (http://n8hpc.org.uk). All one hundred realisations were executed at the same time on one hundred cores using the Oracle Grid Engine. Each realisation used one core. ParaFEM scales on many cores, so larger models can be executed using two tier parallelism. Each realisation can be distributed over several cores and hundreds of realisations can be run at the same time. This simulation strategy is very suited to Cloud Computing [18].

3. Results

It is neither practical nor informative to plot displacement or stress for all one hundred realisations. Instead the authors demonstrate the effect of the spatial variability of material properties by plotting the radial displacement and von Mises stress along a line in the bore running vertically from the top to bottom of the brick (Sections 3.1 And 3.2). The effect on ovality is also mentioned (Section 3.3) and some typical plots are shown for selected realisations (Section 3.4).

3.1. Radial displacement along a line in the bore

Radial displacements along the line in the bore indicated in Fig. 1 are compared in Fig. 7 for the three temperature profiles. Fig. 7a compares the results of the MCS with the deterministic analysis for the uniform temperature change. The radial displacement for the deterministic case is a straight line. All nodes along the line have been displaced 0.28 mm. As the CTE and Young's modulus are the same for all finite elements in the mesh, the brick has expanded uniformly as expected under the uniform temperature change. In contrast, the MCS results for 100 realisations show a scatter of radial displacements from 0.23 mm to 0.34 mm. The spatial variability of CTE and Young's modulus leads to an irregular pattern of displacements along the line. The mean of the MCS results is a straight line with a radial displacement of approximately 0.28 mm. This coincides with the deterministic result and confirms that around 100 realisations are enough to generate statistically reliable results for the mean displacements.

Fig. 7b presents the MCS and deterministic results for the linear gradient temperature change. The radial displacement along the bore is a curved line for the deterministic analysis and the mean of the MCS. This is consistent with an effect known as thermal bowing, produced when a thermal linear gradient is applied to an object. Usmani et al. [32] demonstrate the effect using beam theory and Rapier and Jones [33] describe thermal bowing for reactor fuel elements. The radial displacements calculated using the MCS for 100 realisations range from 0.24 mm to 0.4 mm. This range of displacements is greater than the other cases and arises due to both the thermal bowing and the spatial variation in CTE and Young's modulus.

Fig. 7c concerns the case of a "real" temperature profile. The radial displacements show only slight thermal bowing as the maximum difference in temperature is around 25°. The distribution of values obtained using the MCS is similar to the uniform temperature change (Fig. 7a). Fig. 7d shows radial displacements for three realisations selected from the MCS results computed for the "real" temperature change profile.

3.2. Von Mises stress values along a line in the bore

Fig. 8 shows the von Mises stress values along a line in the bore of the brick. The line selected corresponds exactly with the line used to generate the radial displacement plots in Fig. 7 and both figures may be compared.

Fig. 8a shows that von Mises stress is generated under a homogeneous temperature change when there is spatial variability in CTE and Young's modulus. The values for 100 realizations range from 0.4 to 4.2 MPa. There is no curve for the deterministic case as thermal stresses are not generated in an object with uniform material properties that is allowed to freely expand.

Fig. 8b concerns the linear gradient temperature change. The random spatial variation in CTE and Young's modulus leads to a range of von Mises stress values for 100 realizations from 0.4 to 5.4 MPa. Stress is also generated when the properties are homogeneous as highlighted by the curve for the deterministic case. This is due to the thermal bowing effect.

Fig. 8c presents results for the "real" temperature profile. Small thermal stresses are generated in the deterministic case due to the difference in temperature change across the region of interest. The MCS results give a range of von Mises stress for 100 realizations from 0.4 to 4.2 MPa. Even though the average radial displacement value for the MCS is similar to the value obtained in the deterministic analysis, the von Mises stress values in the MCS are larger.

3.3. Ovality

Physical inspections in working reactors involve measuring distortion around the bore of the brick. The results of the finite element analyses were processed to make similar measurements of

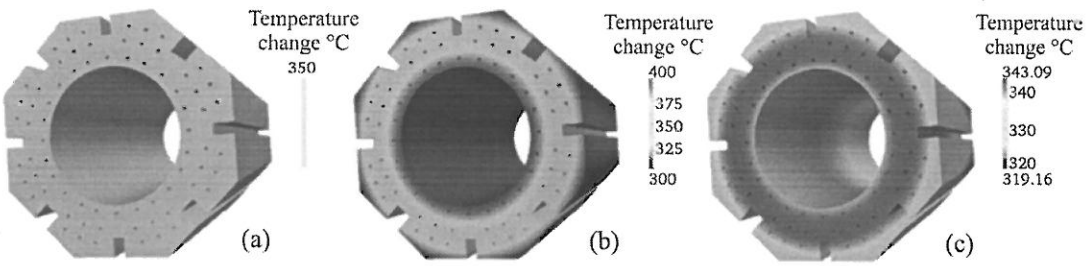

Fig. 6. Temperature profiles used in this research: a) uniform temperature change, b) linear gradient temperature change and c) "real" temperature change.

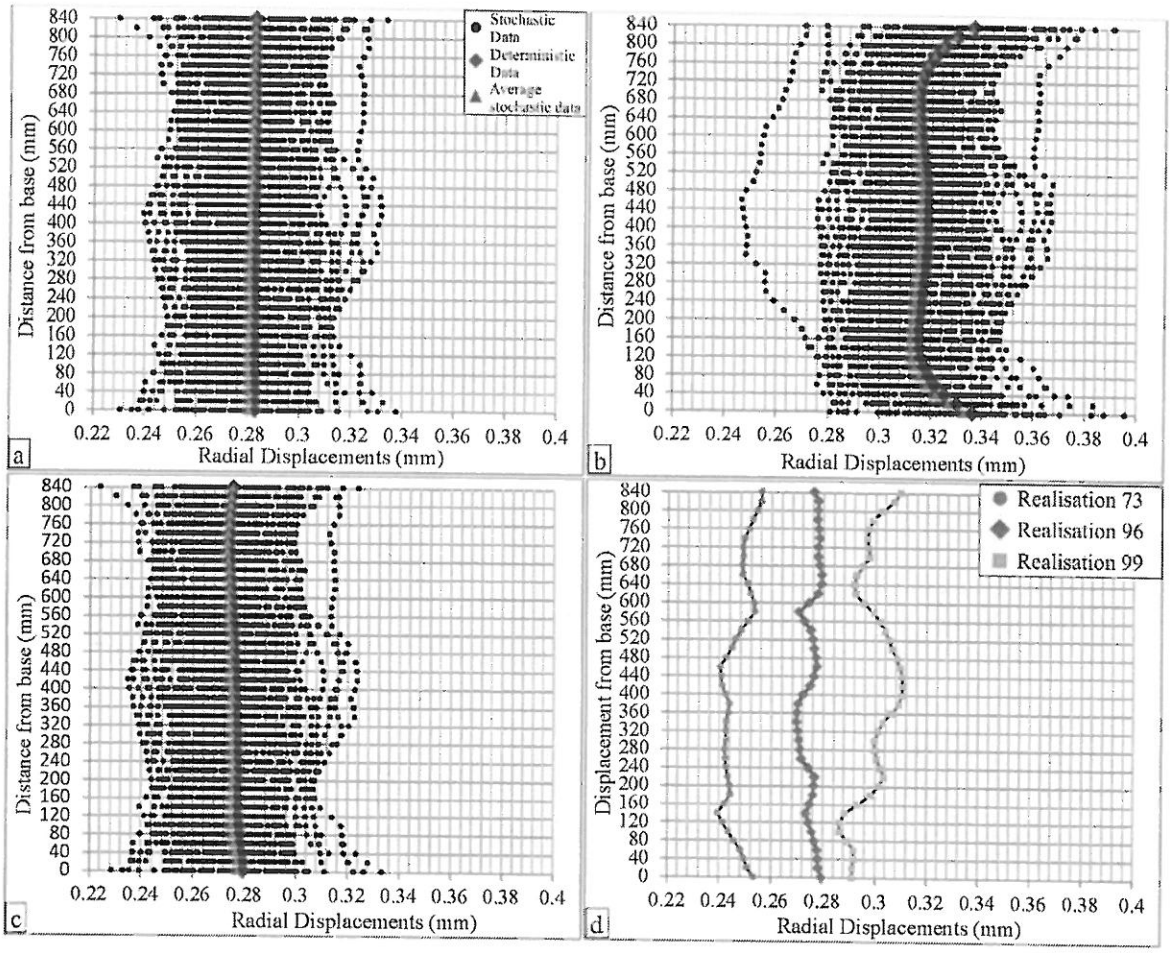

Fig. 7. Radial displacements along a vertical line at the bore of the brick indicated in Fig. 1 for deterministic and stochastic analyses of (a) an homogeneous temperature change, (b) a linear gradient and (c) a "real" profile. Plot (d) shows selected stochastic realizations for the real profile.

ovality. Changes to the circular profile of the bore of the brick were present in the analyses. However, the values were too small (+/− 0.05 mm) to produce a meaningful plot in this paper.

3.4. Von Mises stress in selected realisations

Fig. 9 compares the deterministic analysis of a brick for each of the temperature profiles with the same analyses for one of the selected MCS realisations. The figure shows that stress distribution depends on three factors: features in the geometry; the spatial variability of the material and the temperature profile. In the deterministic case, stress concentrations appear to be related to keyways and corners on the external surface of the brick. In the stochastic plots, the zones of stress concentration are decoupled from the geometry and are instead sensitive to the distribution of material properties. To emphasise this important finding, Fig. 10 shows cross sections for the same three realisations used in Fig. 8. This figure shows that regions with stress concentrations, arising from stochastic material properties, can be generated in any part of the brick.

4. Discussion

4.1. Comparison of deterministic and MCS results

The study presents the influence of spatial variability of bricks subject to three different temperature profiles. When a material is subjected to a temperature change (ΔT) it expands or contracts by a certain amount determined by the CTE. A homogeneous material with a homogeneous rise of temperature that is free to expand does not generate thermal stresses. Under certain conditions, however, thermal stresses may arise. Factors that can cause thermal stresses include temperature gradients, constraining the object of study so that free expansion cannot occur and the presence of material incompatibilities.

This paper has demonstrated that thermal gradients coupled with material incompatibilities may be important in the generation of stress in nuclear graphite reactor bricks. Tiny spatial variations in CTE and Young's modulus can lead to the presence of thermal stresses in bricks that are free to expand. The highest values of von Mises stress computed here are around 4–5 MPa. These values are small and will not lead to cracking. However, the distribution of these initial stress concentrations may be important over the lifetime of a nuclear reactor. They are typically ignored in finite element analyses that are carried out both for reactor design and safety assessment.

Fast neutron irradiation and radiolytic oxidation modify the material properties of graphite and are usually included in computer models via empirical-based fit functions that attempt to map material state to a particular length of operation [34,35]. On initialisation, all the finite elements in these models will have the same mean, deterministic, value for the starting material properties. If

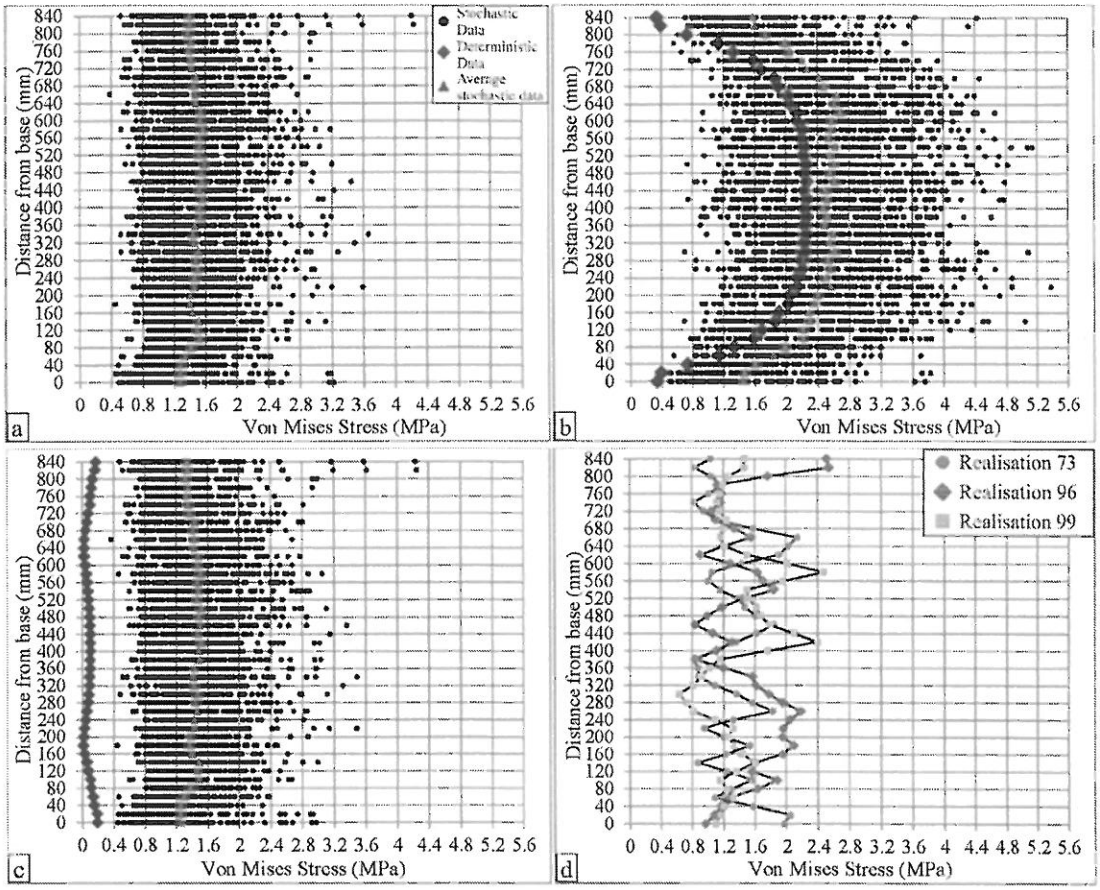

Fig. 8. Von Mises stress computed along a vertical line at the bore of the brick indicated in Fig. 1 for deterministic and stochastic analyses of (a) an homogeneous temperature change, (b) a linear gradient and (c) a "real" profile. Plot (d) shows selected stochastic realisations for the "real" profile.

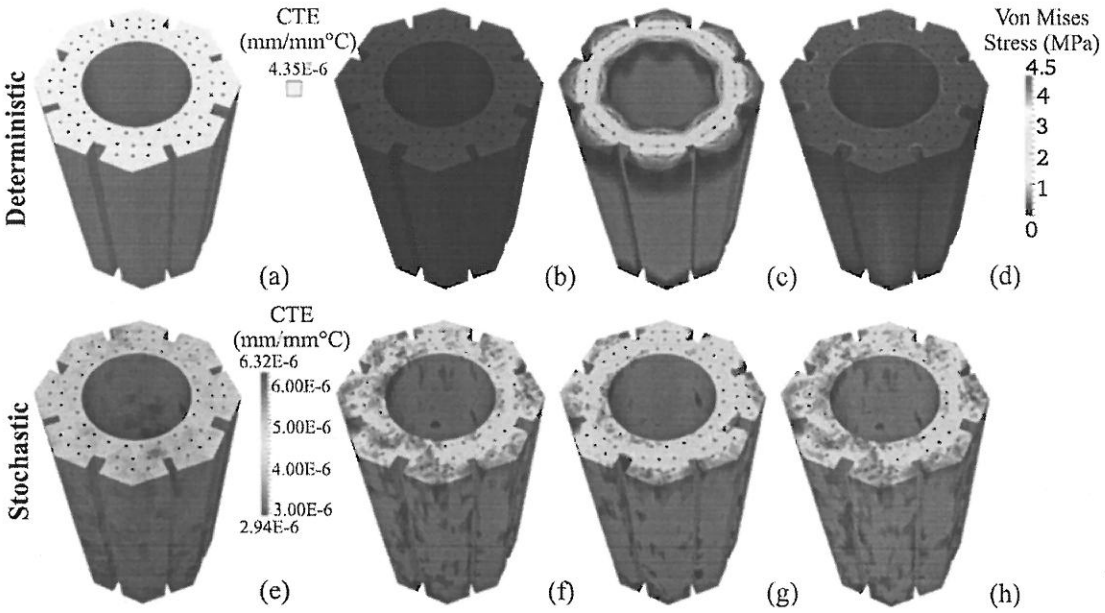

Fig. 9. The effect of spatial variation of CTE and E on von Mises stresses for deterministic and stochastic cases. Individual plots are: (a) Deterministic material properties, (b) Deterministic analysis with a homogeneous temperature change, (c) Deterministic analysis with a linear temperature change, (d) Deterministic analysis with a "real" profile temperature change, (e) Stochastic material properties, (f) Random realisation with a homogeneous temperature change, (g) Random realisation with a linear temperature change, (h) Random realisation with a "real" temperature change.

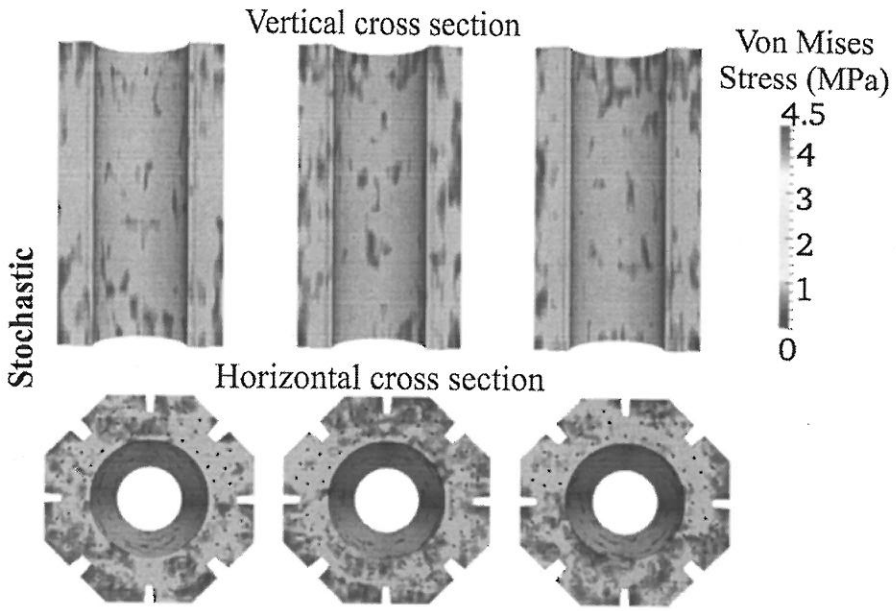

Fig. 10. Von Mises stress distribution of cross sections of three MCS realisations.

spatial variability were to be included, with a slightly different starting value for each finite element, then the historic evolution of material properties in a graphite brick would be different to the deterministic case. Variability may therefore be an important, but overlooked consideration in reactor design and safety assessment. Further study is required to determine whether computer predictions might suggest reactor life would be reduced or extended by more realistic analyses involving MCS.

The deterministic analyses presented here give rise to stress concentrations that coincide with geometric features, such as the keyways. In contrast, the MCS results indicate that stress concentrations may be generated in any part of the brick, decoupled from geometry. Over the lifetime of a reactor, the location of cracking is variable. In the early life of bricks, dimensional change caused by neutron flux is thought to cause stress concentrations in the bore and periphery of the fuel bricks. In later life, high stress concentrations are expected in the keyways. Early cracking may be particularly influenced by initial spatial variability in material properties. Further work is required to investigate the effect of material variability over the lifetime of reactors.

4.2. Effect of number of realisations

The number of realisations required in an MCS is sensitive to the statistical parameters used to generate the random field. Here, a good guide to having carried out enough realisations is when the mean of the displacements obtained using the MCS simulation is close to the value given by the deterministic analysis (which uses the mean value for the material property). We compare displacements because the finite element method solves the system of equations to find the displacements of the nodes in the mesh. For the analyses presented here, 100 realisations were considered to be sufficient for a statistically reliable result as the mean of the MCS displacements was close to the deterministic solution. If the number of realisations is increased, the range of displacements and stress values will not increase in an unbounded manner. An increase in the number of realisations does not necessarily mean that the maximum stress will increase, although it is possible. The highest values of stress are outliers and the majority of the results lie within a fairly well defined band.

4.3. Practical use of MCS for graphite

The findings of the work presented herein may be important in the nuclear industry. However, further work is needed to take this technique beyond the proof of concept stage. Any future studies will require careful calibration of the random fields with better material property data than is currently available. For example, in the case of mechanical properties, we need to determine the mean and standard deviation for a statistically significant number of samples of graphite to characterise the most important material properties. The spatial correlation length for each property is also needed as an input parameter for the random field generator. It can be determined by sampling the material property data at different spatial locations throughout a graphite brick and describing statistically how property values vary within that volume. The process is explained by Dong et al. [22].

Another extension to the work, that could improve the predictive capability of the modelling, involves combining stochastic MCS with the meso-scale modelling of fracture. The ParaFEM software has recently been interfaced with a cellular automata code called CGPACK for multi-scale modelling of fracture in polycrystalline materials [36,37].

5. Conclusions

The authors' modifications to the open source parallel software package ParaFEM have successfully produced a method of incorporating spatial variability of CTE and Young's modulus into a finite element analysis that is repeatedly solved within a Monte Carlo Simulation. The solutions of the new software closely agree with solutions obtained using the commercial software Abaqus and with known analytical solutions to test problems. The MCS results show that tiny spatial variations in CTE and Young's modulus can produce substantial stresses in virgin nuclear graphite bricks under temperature changes that would not produce stresses with uniform values of CTE and Young's modulus.

Acknowledgements

The authors wish to thank the support and resources provided by the Mexican National Science and Technology Council (CONACYT) and the Secretaría de Educación Pública (SEP). This work made use of the facilities of N8 HPC provided and funded by the N8 consortium and EPSRC (Grant No.EP/K000225/1). The Centre is coordinated by the Universities of Leeds and Manchester, UK. The authors gratefully acknowledge the STFC Batteries grant awarded for the project "Random FEM for Energy Applications" which funded a research visit to the Colorado School of Mines.

References

[1] B.J. Marsden, G.N. Hall, 4.11-graphite in gas-cooled reactors, in: R.J.M. Konings (Ed.), Comprehensive Nuclear Materials, Elsevier, Oxford, 2012, pp. 325–390.
[2] G.M. West, S.D.J. McArthur, D. Towle, Nucl. Eng. Des. 241 (9) (2011) 4013–4025.
[3] P.G. Tipping, Understanding and Mitigating Ageing in Nuclear Power Plants [electronic Resource] : Materials and Operational Aspects of Plant Life Management (PLiM), Woodhead Publishing; Oxford, Philadelphia, 2010, p. 1 online resource (xxxvii, 914).
[4] D.K.L. Tsang, B.J. Marsden, J. Nucl. Mater. 350 (3) (2006) 208–220.
[5] D.K.L. Tsang, B.J. Marsden, J. Nucl. Mater. 381 (1–2) (2008) 129–136.
[6] S. Mohanty, S. Majumdar, M. Srinivasan, Nucl. Eng. Des. 260 (2013) 145–154.
[7] S.Y. Yu, X. Fang, H.T. Wang, C.F. Li, Nucl. Eng. Des. 253 (2012) 192–199.
[8] K.Y. Wen, T.J. Marrow, B.J. Marsden, Carbon 46 (1) (2008) 62–71.
[9] G. Hall, B.J. Marsden, S.L. Fok, J. Nucl. Mater. 353 (1–2) (2006) 12–18.
[10] M. Carroll, J. Lord, D. Rohrbaugh, Baseline Graphite Characterization: First Billet, INL/EXT-10-19810 TRN: US1100212, Idaho National Laboratory, United States, 2010.
[11] C.R. Kennedy, O.R.N. Laboratory, Statistical Characterization of Three Grades of Large Billet-graphites: Stackpole 2020, Union Carbide TS1792, and Toyio Tanso IG11; DE2001-770926, Technical Information Center, Oak Ridge Tennessee, 1987, p. p 72.
[12] J.P. Strizak, Spatial Variability in the Tensile Strength of an Extruded Nuclear-grade Graphite, International Atomic Energy Agency (IAEA), Austria, 1993, pp. 64–69.
[13] S.D. Preston, The Statistical Variation Present in the Material Properties of Dungeness, Hartlepool, Heysham I and Heysham II/Torness CAGR Moderator Graphites ND-M-3008(S), United Kingdom Atomic Energy Authority Northern Division, 1986.
[14] S.D. Preston, Variation of Material Properties within a Single Brick of the Heysham 2/Torness Moderator Graphite; ND-M-3755(S), United Kingdom Atomic Energy Authority Northern Division, 1988.
[15] B.C. Mitchell, Understanding and Development of Nuclear Graphite Technology, PhD, The University of Manchester, Manchester, 2003.
[16] J.P. Strizak, Spatial Variability in the Tensile Strength of an Extruded Nuclear-grade Graphite, Technical Information Center, Oak Ridge Tennessee, 1991.
[17] J. Arregui-Mena, L. Margetts, P. Mummery, Arch. Comput. Methods Eng. (2014) 1–20.
[18] I.M. Smith, D.V. Griffiths, L. Margetts, Programming the Finite Element Method, fifth ed., Wiley, Chichester, West Sussex, United Kingdom, 2014.
[19] G.A. Fenton, D.V. Griffiths, Risk Assessment in Geotechnical Engineering, John Wiley & Sons, Inc., Chichester, 2008. John Wiley [distributor]: Hoboken, N.J.
[20] D.V. Griffiths, G.A. Fenton, Geotechnique 43 (4) (1993) 577–587.
[21] G.A. Fenton, D.V. Griffiths, Cism Courses Lect. 491 (2007) 201–223.
[22] X.N. Dong, Q. Luo, D.M. Sparkman, H.R. Millwater, X. Wang, Bone 47 (6) (2010) 1080–1084.
[23] E.H. Isaaks, R.M. Srivastava, Applied Geostatistics, Oxford University Press, 1989.
[24] K.H. Huebner, The Finite Element Method for Engineers, Wiley-Interscience, New York ; London, 1975, p. xix,500.
[25] D.S. Burnett, in: Finite Element Analysis : from Concepts to Applications, Repr. With Corrections, Addison-Wesley Pub. Co., Reading, Mass. ; Wokingham, England, 1988 xix, 844 pages.
[26] K. Hibbitt, Sorensen, ABAQUS/CAE User's Manual, Hibbitt, Karlsson & Sorensen, Incorporated, 2006.
[27] A.C. Davies, The Science and Practice of Welding, sixth ed., Cambridge University Press, London, 1972, p. xi, 590.
[28] R.C. Hibbeler, Mechanics of Materials, eighth ed., Pearson Prentice Hall, Upper Saddle River, N.J, 2011, p. xv, 862.
[29] I.M. Smith, L. Margetts, Eng. Comput. 23 (1–2) (2006) 154–165.
[30] S. Yoda, K. Fujisaki, J. Nucl. Mater. 113 (2–3) (1983) 263–267.
[31] AMEC PANTHER - An Advanced 3D Nodal Code for Reactor Core Analysis. http://www.answerssoftwareservice.com/panther/(accessed 01.08. 14).
[32] A.S. Usmani, J.M. Rotter, S. Lamont, A.M. Sanad, M. Gillie, Fire Saf. J. 36 (8) (2001) 721–744.
[33] A.C. Rapier, T.M. Jones, J. Nucl. Energy Ab. 19 (1965) (3pa-), 145-&.
[34] E.D. Eason, G.N. Hall, B.J. Marsden, C.B. Heys, J. Nucl. Mater. 436 (1–3) (2013) 201–207.
[35] E.D. Eason, G.N. Hall, B.J. Marsden, C.B. Heys, J. Nucl. Mater. 436 (1–3) (2013) 191–200.
[36] A. Shterenlikht, L. Margetts, Proc. R. Soc. Lond. A: Math. Phys. Eng. Sci. 471 (2177) (2015).
[37] A. Shterenlikht, L. Margetts, L. Cebamanos, D. Henty, SIGPLAN Fortran Forum 34 (1) (2015) 10–30.